THE JOURNAL OF PHYSICAL CHEMISTRY A LETTERS

2009, *113,* 9579–9584
Published on Web 07/17/2009

Observation of a Remarkable Temperature Effect in the Hydrogen Bonding Structure and Dynamics of the $CN^-(H_2O)$ Cluster

Xue-Bin Wang,[†] Jasper C. Werhahn,[‡] Lai-Sheng Wang,*[,†] Karol Kowalski,[§] Alfred Laubereau,[‡] and Sotiris S. Xantheas*[,∥]

Department of Physics, Washington State University, 2710 University Drive, Richland, Washington 99354, Chemical & Materials Sciences Division, Pacific Northwest National Laboratory, 902 Battelle Boulevard, P.O. Box 999, MS K8-88, Richland, Washington 99352, Environmental Molecular Sciences Laboratory, Pacific Northwest National Laboratory, P.O. Box 999, MS K8-91, Richland, Washington 99352, Physik-Department E11, Technische Universität München, James-Franck-Strasse, D-85748 Garching, Germany, and Chemical & Materials Sciences Division, Pacific Northwest National Laboratory, 902 Battelle Boulevard, P.O. Box 999, MS K1-83, Richland, Washington 99352

Received: April 13, 2009; Revised Manuscript Received: June 24, 2009

The $CN^-(H_2O)$ cluster represents a model diatomic monohydrate with multiple solvation sites. We report joint experimental and theoretical studies of its structure and dynamics using temperature-controlled photoelectron spectroscopy (PES) and ab initio electronic structure calculations. The observed PES spectra of $CN^-(H_2O)$ display a remarkable temperature effect, namely that the $T = 12$ K spectrum shows an unexpectedly large blue shift of 0.25 eV in the electron binding energy relative to the room temperature (RT) spectrum. Extensive theoretical analysis of the potential energy function (PEF) of the cluster at the CCSD(T) level of theory reveals the existence of two nearly isoenergetic isomers corresponding to H_2O forming a H-bond with either the C or the N atom, respectively. This results in four topologically distinct minima, i.e., $CN^-(H_aOH_b)$, $CN^-(H_bOH_a)$, $NC^-(H_aOH_b)$, and $NC^-(H_bOH_a)$. There are two main pathways connecting these minima: (i) CN^- tumbling relative to water and (ii) water rocking relative to CN^-. The relative magnitude of the barriers associated with these two motions reverses between low (pathway i is preferred) and high (pathway ii is preferred) temperatures. As a result, at $T = 12$ K the cluster adopts a structure that is close to the minimum energy $CN^-(H_2O)$ configuration, while at RT it can effectively access regions of the PEF close to the transition state for pathway ii, explaining the surprisingly large spectral shift between the 12 K and RT PES spectra.

I. Introduction

Gas phase clusters of simple ions solvated with a controlled number of solvent molecules are ideal models in obtaining microscopic insight into the properties of aqueous electrolyte solutions.[1−4] Many gas phase experimental techniques[5−12] as well as theoretical approaches[13−17] have been used to study solvated clusters. Temperature plays a key role in the spectroscopy of solvated clusters,[18] and various cooling techniques such as argon tagging[11,12] or helium nanodroplets[19,20] have been the driving forces for the recent resurgence of the field. Most of the research efforts on solvated ions have been devoted to relatively simple cations or anions using Ar-tagging predissociation.[11,12] Recent advances in ion trap technology have made it possible to produce cold ions down to very low temperatures[21] and to allow for spectroscopic studies of microsolvated complexes and multiply charged ions under well-controlled temperatures.[22−24]

Monohydrate anions, such as $Cl^-(H_2O)$, have drawn particular attention due to their simplicity and role as prototypes to understand ion−water interactions.[10,11,15,18,25,26] Temperature effects cannot be more emphasized than those appeared in two previous experimental infrared (IR) action spectra by Okumura[10] and Johnson[11] on $Cl^-(H_2O)$, where, although similar vibrational frequencies were observed, the respective intensities were completely different, apparently due to the different temperatures of the clusters.[18] It is surprising that no gas phase spectroscopic studies have been reported to date on $CN^-(H_2O)_n$ clusters, considering the ubiquity and wide applications of cyanide anions in solutions and solids. Despite the fame of being a "pseudohalide", the cyanide anion is quite different from the halides in its hydration mechanism as it can form two H-bonded complexes with water via either the C or the N side.[27] The study of $CN^-(H_2O)_n$ clusters, therefore, not only yields details about the microscopic molecular interactions between CN^- and H_2O but also provides a case for comparison with the halide solvation.

In this study we present a joint experimental/theoretical study of the H-bonding structure and dynamics of $CN^-(H_2O)$ by temperature-controlled PES and high-level ab initio electronic

* Corresponding authors. E-mail: L.-S.W., ls.wang@pnl.gov; S.S.X., sotiris.xantheas@pnl.gov.
[†] Washington State University and Chemical & Materials Sciences Division (MS K8-88), Pacific Northwest National Laboratory.
[‡] Technische Universität München.
[§] Environmental Molecular Sciences Laboratory, Pacific Northwest National Laboratory.
[∥] Chemical & Materials Sciences Division (MS K1-83), Pacific Northwest National Laboratory.

10.1021/jp9034002 CCC: $40.75

structure calculations. PES spectra were obtained at two temperatures (12 K and RT), probing the ground and first excited states of $CN(H_2O)$, as well as the $CN^-(H_2O)^+$ charge-transfer state. Comparison between the 12 K and RT spectra revealed a surprisingly large blue shift of 0.25 eV in electron binding energies. High level ab initio calculations identified two almost isoenergetic minima, corresponding to $CN^-(H_2O)$ and $NC^-(H_2O)$, and two intermolecular soft motions of water rocking and CN^- tumbling to connect these two minima. The calculations yield converged (with regard to the level of electron correlation and orbital basis set) vertical detachment energies (VDEs) to the ground and excited states of the neutral cluster that are in quantitative agreement with the experiment and unravel the origin of the energy shift observed at RT due to the sampling of different cluster configurations.

II. Approach

Experimental Section. The experiments were performed using two home-built apparatuses that couple an electrospray ionization (ESI) source to a magnetic-bottle time-of-flight photoelectron spectrometer. The $CN^-(H_2O)$ cluster was generated via electrospray from a 1 mMol NaCN solution in a water/acetonitrile mixed solvent. The RT experiment was carried out in an ESI-PES instrument that has been described in detail elsewhere,[28] while the $T = 12$ K data were obtained using a newly developed instrument that has the ability to cool ions to low temperatures.[29] In this case the anions produced from the ESI source were guided by two RF-only devices and a 90° ion bender into a Paul trap, which is attached to the cold head of a closed-cycle helium cryostat. In the current experiment the ion trap was operated at 12 K and ions were collisionally cooled for 0.1 s by a 1 mTorr background gas (He/20% H_2) before being pulsed out into the extraction zone of a time-of-flight mass spectrometer.

During each PES experiment, the anions of interest were mass selected and decelerated before being intercepted by a detachment laser beam in the interaction zone of a magnetic-bottle photoelectron analyzer. The spectra of the $CN^-(H_2O)$ anion were obtained at 193 nm (6.424 eV) from an ArF excimer laser. Photoelectron time-of-flight spectra were measured and then converted into kinetic energy spectra, calibrated by the known spectra of I^- and ClO_2^-. The electron binding energy spectra were obtained by subtracting the kinetic energy spectra from the detachment photon energy. The energy resolution ($\Delta E/E$) was estimated to be approximately 2%, i.e., approximately 20 meV for 1 eV electrons.

Electronic Structure Calculations. The stationary points (minima, transition states) were fully optimized at the second-order Moller−Plesset (MP2) and coupled-cluster singles and doubles with perturbative estimate of triple excitations [CCSD(T)] levels of theory using the family of augmented correlation consistent basis sets, aug-cc-pVnZ (n = D, T, Q), of Dunning and co-workers.[30] All MP2 calculations were performed with the Gaussian 98 suite of codes,[31] whereas all CCSD(T) calculations were carried out with the NWChem suite of electronic structure codes.[32] All open-shell coupled-cluster calculations, needed for the calculation of the VDEs, were based on a doublet restricted open-shell Hartree−Fock reference with the core electrons being frozen. These calculations were performed using the tuned tensor contraction engine (TCE)[33] implementation of the CCSD[34] and CCSD(T)[35] approaches (for details and scalability analysis see ref 36) implemented within the NWChem suite of electronic structure codes.[32] The best estimates for the energy difference between the two minima were obtained at the CCSD(T)/aug-cc-pVQZ level of theory (332 basis functions) with ZPE corrections estimated at the CCSD(T)/aug-cc-pVTZ level. For the transition states, CCSD(T)/aug-cc-pVQZ single point energies were obtained at the CCSD(T)/aug-cc-pVDZ optimal geometries, which were also used to estimate ZPE corrections. To better visualize the interconversion pathways between the various stationary points of the $CN^-(H_2O)$ cluster, a reduced PEF as a function of the two angles defining the orientation of the CN fragment relative to H_2O (vide supra) was produced. The calculations to obtain the reduced PEF were performed at the CCSD(T)/aug-cc-pVDZ level with the MOLPRO suite of electronic structure codes.[37]

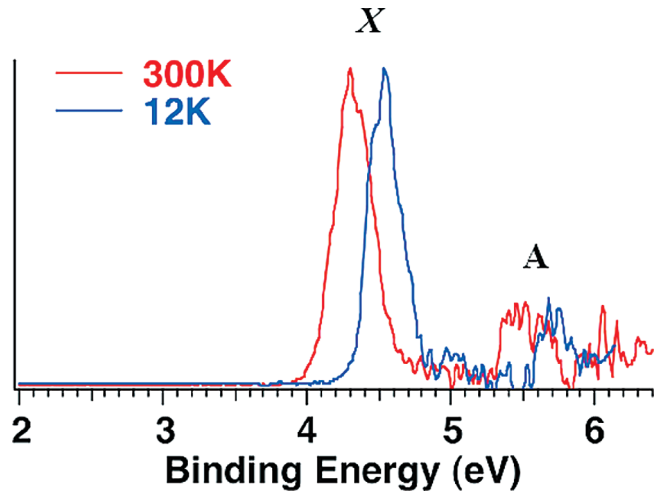

Figure 1. Photoelectron spectra of $CN^-(H_2O)$ at 193 nm (6.424 eV) at 12 K and room temperature.

III. Results

Photoelectron Spectroscopy. We carried out the PES study of $CN^-(H_2O)$ using a home-built magnetic bottle time-of-flight PES apparatus that couples an electrospray ionization (ESI) source and a temperature-controlled ion-trap.[28,29] The $CN^-(H_2O)$ cluster was generated via ESI and mass-selected before exposure to the detachment light. Figure 1 shows the 193 nm PES spectra of $CN^-(H_2O)$ at 12 K (blue) and RT (red).[38] Two main features are observed at $T = 12$ K: an intense peak (X) centered at 4.54 eV (Table 1) and a weaker one (A) at ~5.7 eV. At RT, a surprisingly large red shift in electron binding energies of 0.25 eV is observed, while the overall spectral pattern and widths are largely unchanged. We also measured the PES spectrum of the bare CN^- anion at 266 nm (4.661 eV) that shows one single sharp peak with a VDE of 3.85 eV (Table 1). This result is consistent with a previous high-resolution study,[39] which observed only the 0−0 transition at 266 nm, and yielded an adiabatic detachment energy (ADE) or VDE of 3.862 eV. The current CN^- spectrum confirmed the proper calibrations under which the $CN^-(H_2O)$ spectra were taken. The apparent broadness of the $CN^-(H_2O)$ spectra should be due to solvent relaxation upon electron detachment.

The $T = 12$ K spectrum shows that a single water molecule stabilizes the negative ion by 0.69 eV. Since the first excited state of CN (neutral) lies 1.146 eV above the ground state,[40] the observed weak feature (peak A at ~5.7 eV, 1.16 eV higher relative to X) should correspond to the excited state of CN solvated by one water molecule.

Global Minimum of the $CN^-(H_2O)$ Cluster and Calculated VDEs. We first benchmarked various theoretical methods for the bare CN^- anion. The change in the equilibrium separation

TABLE 1: Minimum Energies (au) of Anion Optimized Geometries and Single Point Energies of the Corresponding Neutral Species, Relative Energies (kcal/mol) between the $CN^-(H_2O)$ and $NC^-(H_2O)$ Isomers (Including Harmonic ZPE Corrections in Parentheses), Calculated VDEs (eV) and Their Comparison with Experimentally Measured Values

species	level of theory	basis set	anion au	ΔE_e (ΔE_0), kcal/mol	neutral au	VDE (calc), eV	VDE (exp), eV
CN	MP2	aug-cc-pVDZ	−92.620710		−92.469284	4.12	
		aug-cc-pVTZ	−92.693083		−92.536676	4.26	
		aug-cc-pVQZ	−92.718157		−92.559560	4.32	
	CCSD(T)	aug-cc-pVDZ	−92.640527		−92.505948	3.66	
		aug-cc-pVTZ	−92.713105		−92.573408	3.80	
		aug-cc-pVQZ	−92.735399		−92.594279	**3.84**	**3.862 ± 0.004**[a]
$CN(H_2O)$	MP2	aug-cc-pVDZ	−168.907047	0	−168.731696	4.77	
		aug-cc-pVTZ	−169.047976	0	−168.867283	4.92	
		aug-cc-pVQZ	−169.095706	0	−168.912780	4.98	
	CCSD(T)	aug-cc-pVDZ	−168.939643	0	−168.779454	4.36	
		aug-cc-pVTZ	−169.081178	0	−168.915780	4.50	
		aug-cc-pVQZ	−169.124410	0	−168.957592	**4.54**	**4.54 ± 0.05**
$NC(H_2O)$	MP2	aug-cc-pVDZ	−168.906902	0.09 (−0.03)	−168.722967	5.01	
		aug-cc-pVTZ	−169.047973	0.00 (−0.12)	−168.858387	5.16	
		aug-cc-pVQZ	−169.095706	0.00 (−0.12)	−168.903781	5.22	
	CCSD(T)	aug-cc-pVDZ	−168.939027	0.39 (0.37)	−168.774585	4.47	
		aug-cc-pVTZ	−169.080756	0.26 (0.21)	−168.910603	4.63	
		aug-cc-pVQZ	−169.124003	0.26 (0.21)	−168.952249	**4.67**	

[a] From ref 39.

between the neutral and the anion is minimal, viz. $R_e = 1.1814$ Å (CN^-) and 1.1753 Å (CN) at the CCSD(T)/aug-cc-pVQZ level of theory, is in accord with the fact that only the 0−0 transition is observed in the PES spectra of CN^-. The calculated VDEs are listed in Table 1 at the MP2 and CCSD(T) levels of theory. As a general rule, MP2 was found to overestimate the VDE by as much as 0.5 eV, whereas CCSD(T) produces a very accurate value of 3.84 eV with the aug-cc-pVQZ basis set, just ∼0.02 eV shy of the experimental value. The variation of the CCSD(T) results with basis set further suggests that the value obtained with the aug-cc-pVQZ set is converged to within ∼0.02 eV from the complete basis set (CBS) limit.

For the $CN^-(H_2O)$ cluster we identified two almost isoenergetic H-bonded isomers, noted as $CN^-(H_2O)$ and $NC^-(H_2O)$, which correspond to the anion binding to one of the hydrogen atoms of water with either the N or the C atoms, respectively. The relative energies of these two isomers at the MP2 and CCSD(T) levels of theory with the aug-cc-pV*n*Z (n = D, T, Q) basis sets are shown in Table 1. We note that at the MP2 level of theory the two isomers are isoenergetic to within <0.01 kcal/mol, whereas the inclusion of harmonic zero-point energy (ZPE) estimates incorrectly (vide infra) stabilizes the $NC^-(H_2O)$ isomer by 0.12 kcal/mol. However, the situation is reversed upon geometry reoptimization at the CCSD(T) level of theory, which identifies the $CN^-(H_2O)$ isomer as the more stable one by as much as 0.21 kcal/mol (including harmonic ZPE estimates at the CCSD(T)/aug-cc-pVTZ level, cf. Table 1), whereas thermal corrections to the enthalpy at RT slightly increase this energy difference to 0.24 kcal/mol. This finding is consistent with the fact that the calculated VDE for the $CN^-(H_2O)$ isomer (4.54 eV, cf. Table 1) converges to the experimental value within the experimental uncertainty, whereas for the $NC^-(H_2O)$ isomer the calculated value is 0.13 eV higher. The excellent agreement between the experiment and theory confirms unambiguously that the $CN^-(H_2O)$ isomer is the global minimum on the potential energy function (PEF). As is the case for the bare anion, we also find that for the monohydrate cluster the MP2 level of theory overestimates the VDE by as much as 0.4 eV compared to CCSD(T) (cf. Table 1).

In addition, two excited states of the $CN(H_2O)$ neutral cluster are found, one with excitation entirely localized on the CN fragment, noted as $CN^*(H_2O)$ with a calculated excitation energy of 1.34 eV and a VDE of 5.88 eV, the other of charge-transfer character from the O atom of the water moiety to the C atom, noted as $CN^-(H_2O)^+$, with a calculated excitation energy of 1.32 eV and a VDE of 5.86 eV. Both calculated VDEs are in good accord with the experimentally observed (A) band at ∼5.7 eV at T = 12 K (cf. Figure 1), suggesting that the A band should contain contributions from both excited states.

IV. Discussion

Ground State Potential Energy Function of $CN^-(H_2O)$. The optimal structures of the various stationary points (two minima, three first- and one second-order transition states) on the ground state PEF of $CN^-(H_2O)$ and their connectivity are schematically shown in Figure 2. Their energies [relative to the $CN^-(H_2O)$ global minimum (M)] and associated barriers at 0

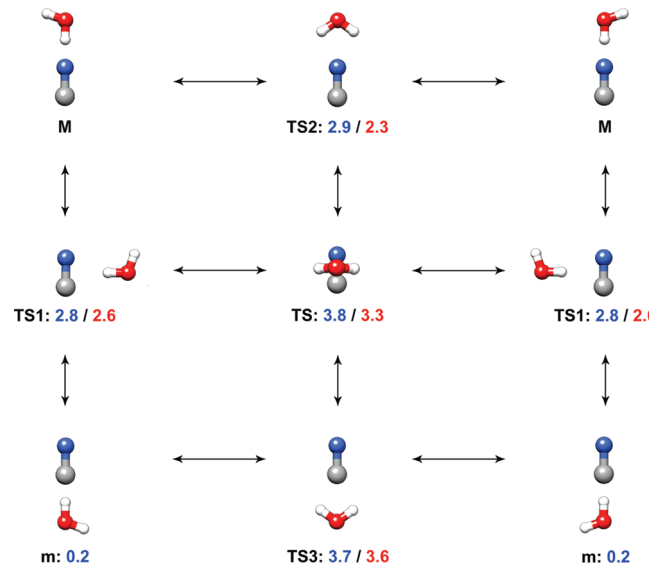

Figure 2. Stationary points and their connectivity on the ground state potential energy function of $CN^-(H_2O)$. Relative energies (in kcal/mol, including harmonic zero-point energy corrections) for 0 K (blue) and room temperature (red) at the CCSD(T)/aug-cc-pVQZ level of theory are given with respect to the global minimum (M). Key: blue, N; gray, C; red, O; white, H.

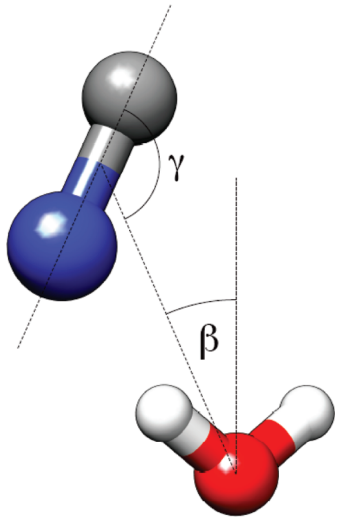

Figure 3. Definition of the angles β and γ that describe the relative orientation of the CN fragment with respect to H_2O.

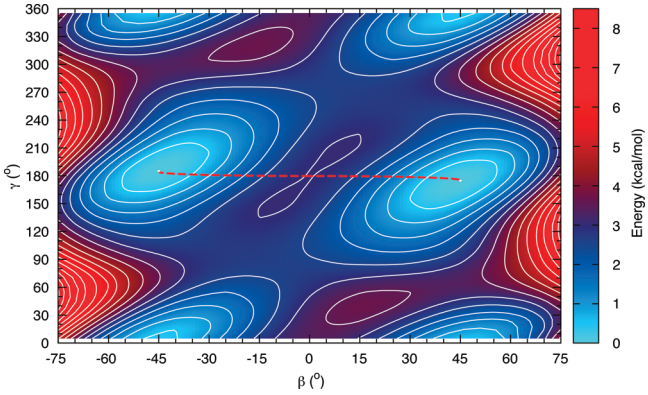

Figure 4. Reduced potential energy function for the ground state of $CN^-(H_2O)$ as a function of the angles β and γ defined in Figure 3. For each value of (β, γ) the rest of the seven internal coordinates were optimized at the CCSD(T)/aug-cc-pVDZ level of theory. Contours are drawn with a 0.5 kcal/mol increment.

K (blue) and RT (red) are shown at the CCSD(T)/aug-cc-pVQZ level of theory including harmonic ZPE corrections with the aug-cc-pVDZ basis set. We have identified three first order transition states (each having only one imaginary frequency) corresponding to the $CN^-(H_2O) \leftrightarrow NC^-(H_2O)$ interconversion (TS1) and the isomerizations between the $CN^-(H_2O)$ (TS2) and $NC^-(H_2O)$ minima (TS3), respectively. A second-order (having two imaginary frequencies) transition state (TS) interconnects the two equivalent structures of TS1 and also the pathway between TS2 and TS3, as indicated by the arrows in Figure 2. In general, the CCSD(T) barriers were found to be 10−20% higher than the corresponding ones computed at the MP2 level of theory.

To obtain a quantitative picture of the interconversion pathways between the stationary points, we have devised a reduced representation of the full 9-dimensional PEF in terms of the angles β and γ that define the orientation of the CN fragment relative to the H_2O molecule, as shown in Figure 3. For each (β, γ) pair on this reduced PEF, all the other seven internal coordinates of the cluster were optimized at the CCSD(T)/aug-cc-pVDZ level. The angles β and γ were varied in 5° increments whereas because of symmetry $V(\beta,\gamma) = V(-\beta, 360 - \gamma)$. The resulting reduced PEF is shown in Figure 4 where the contours are drawn with a 0.5 kcal/mol increment. It should be noted that the barriers associated with this reduced PEF are at the CCSD(T)/aug-cc-pVDZ level of theory and differ from the best estimates at the CCSD(T)/aug-cc-pVQZ (including harmonic ZPE corrections at the CCSD(T)/aug-cc-pVDZ) level of theory shown in blue in Figure 2.

Effect of Temperature on the Ground State PEF and PES Spectra. At $T = 0$ K the lowest barrier is the one associated with TS1 ($\Delta E_0 = 2.8$ kcal/mol, cf. Figure 2) corresponding to the interconvesion between the $CN^-(H_2O)$ and $NC^-(H_2O)$ minima via the tumbling of CN^- with respect to water (pathway i). However, the inclusion of harmonic corrections to the enthalpy of the cluster at RT changes this picture as it suggests a lower pathway ii associated with the rocking motion of water via TS2 ($\Delta H^{298K} = 2.3$ kcal/mol) indicated by the broken red line in Figure 4. The other barriers at RT (denoted by red in Figure 2) are 2.6 kcal/mol (TS1), 3.6 kcal/mol (TS3), and 3.3 kcal/mol (TS). Inclusion of these harmonic corrections further alters the "0 K" picture of the PEF shown in Figure 2, because, for example, they place the second-order transition state (TS) 0.3 kcal/mol below TS3. Although the TS1 and TS2 barriers are similar in height, the effective masses are quite different: the tumbling via TS1 involves the movement of the entire H_2O fragment relative to CN whereas the rocking via TS2 involves just the wiggling of the protons leaving the three heavy atoms practically at rest. To this end, TS2 is a much easier barrier to breach and in the following we will concentrate our discussion to the motion of the water molecule via TS2.

The harmonic frequency for the motion that interconverts the global minimum (M) via TS2 (red broken line in Figure 4) is 447 cm^{-1}. A full anharmonic calculation based on higher energy derivatives[41] performed with the Gaussian 03 electronic structure programs[42] yields an anharmonic frequency of 418.5 cm^{-1} for that mode. Using that value for the separation between the $v = 0$ and $v = 2$ levels (levels 0,1 and 1,2 are nearly degenerate, vide infra), we have fitted a quartic potential of the type $V = A\beta^4 + B\beta^2 + C$ to the path indicated with a red broken line in Figure 4 that is associated with a barrier of 2.3 kcal/mol (since this is the preferred path at RT, see previous discussion and Figure 2). From Figure 4 it is also evident that the approximation of a 1-dimensional potential in β is quite realistic as γ is almost constant (to <5°) along this path. The resulting vibrational levels are 282.4 ($v = 0$), 283.9 ($v = 1$), 700.6 ($v = 2$), 759.0 ($v = 3$), and 1022.7 ($v = 4$) cm^{-1}. The levels $v = 0$ and $v = 1$ are almost degenerate and together with the next 2 levels ($v = 2$ and $v = 3$) are below the barrier of 2.3 kcal/mol (or 804 cm^{-1}) whereas the next level ($v = 4$) is above the barrier. The $v = 0 \rightarrow 1$ splitting of 1.5 cm^{-1} matches exactly the tabulated solutions of the Schrödinger equation for a quartic potential,[43,44] whereas the $v = 0 \rightarrow 2$ transition of 418.2 cm^{-1} also exactly matches the computed anharmonic frequency (418.5 cm^{-1}) of the mode that leads to TS2. The vibrational levels and the corresponding probabilities for the $v = 0$ and $v = 2$ levels are shown in Figure 5 along with the path that interconverts the two minima. Again we used our best estimate of 2.3 kcal/mol for the barrier at RT for this analysis, a value that is lower than the one shown in the 2-D PEF that was obtained at the CCSD(T)/aug-cc-pVDZ level (at $T = 0$ K).

While at low temperatures the cluster adopts a structure that is close to the global minimum $CN^-(H_2O)$ configuration ($\beta = \pm 45°$), it can effectively access other regions of the PEF at higher temperatures. For instance, at the first excited vibrational level ($v = 2$) the maxima of the square of the wave function is at $\beta = \pm 22.5°$ and $\pm 52.5°$ (as seen from Figure 5), whereas there is also substantial probability at the TS2 geometry ($\beta = 0°$). The $v = 2$ vibrational level has a Boltzman factor of 0.14

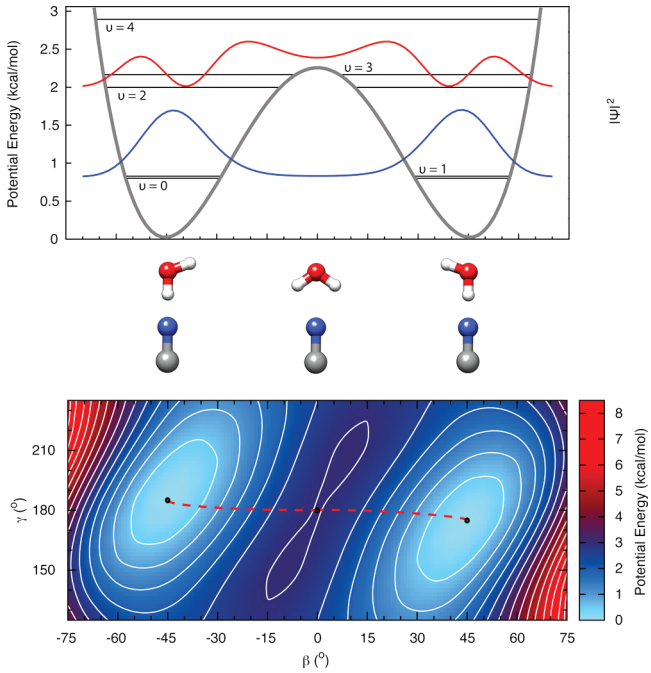

Figure 5. Lowest energy path (red broken line) and energy levels at RT.

at RT. This finding can explain the large electron binding energy shift observed at the low and room temperatures. This assertion is also reinforced from the following results. The calculated VDEs at the two lowest transition states are 4.42 eV (TS1) and 4.36 eV (TS2). Compared to the VDE of 4.54 eV observed at 12 K, these correspond to red shifts of 0.12 eV (for TS1) and 0.18 eV (for TS2). The calculated red shift for TS2 (0.18 eV) is consistent with the observed red shift of 0.25 eV at RT, and it is also consistent with the fact that the estimated barrier associated with that transition state (TS2) is the lowest at RT (cf. Figure 2, barriers indicated in red). Furthermore, the calculated VDEs for the geometries having $\beta = \pm 22.5°$ and $\pm 52.5°$ (maxima of $|\psi|^2$ for $\upsilon = 2$) are 4.38 and 4.49 eV, respectively.

The current results can be put in perspective with the previous controversy regarding the IR spectra of the $Cl^-(H_2O)$ cluster observed by Okumura[10] at RT and by Johnson[11] at low temperatures using Ar tagging. Their IR spectra are totally different at first glance: although similar features (at 3156 and 3285 cm^{-1} by Okumura; 3130 and 3283 cm^{-1} by Johnson) were observed, their relative intensities were completely different. While the 3285 cm^{-1} feature was dominant in the RT experiments, that peak became quite weak at low temperatures and instead the 3130 cm^{-1} peak became dominant in the low temperature IR spectrum. Theoretical calculations assigned the 3130 cm^{-1} peak as the ionic hydrogen-bonding OH stretch, and the 3283 cm^{-1} feature to the bend overtone of H_2O. As shown in Figure 6, the minimum energy configuration of $Cl^-(H_2O)$ tends to optimize the chloride interaction with one H atom of the water moiety resulting in a C_s structure (giving rise at an elongated OH bond that results in the red shift of the corresponding OH stretch), whereas the transition state corresponding to the water rocking motion is a bifurcated C_{2v} structure with a 1.3 kcal/mol barrier (at the MP2/aug-cc-pVDZ level including ZPE corrections) with a substantially smaller H−O−H bond angle.[15] The stark contrast of the $Cl^-(H_2O)$ IR spectra indicate that the ionic OH stretching mode is excited in the low temperature data because the cluster adopts the C_s geometry,

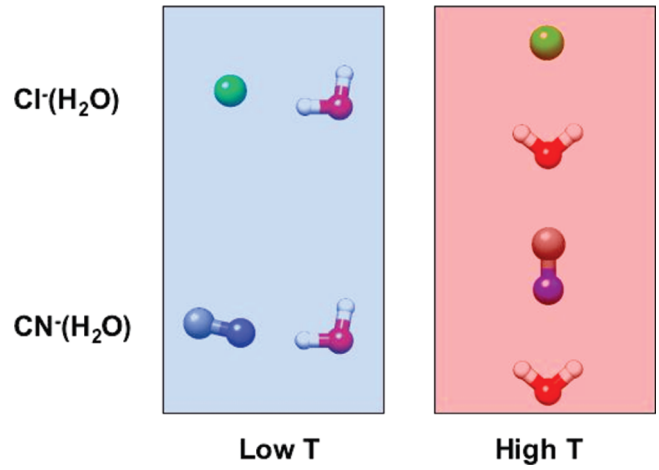

Figure 6. Representative configurations of the $Cl^-(H_2O)$ and $CN^-(H_2O)$ clusters at low and high T (green, Cl; gray, C; blue, N; red, O; white, H).

whereas the water bending mode is activated in the RT spectrum because the cluster can access configurations that are near the transition state configuration at high temperatures. Our results indicate that the ground state PEF of $CN^-(H_2O)$ parallels that of $Cl^-(H_2O)$ (Figure 6). While the low temperature PES spectrum reflects the detachment of an electron from the global minimum, the RT spectrum more likely corresponds to detaching an electron from a configuration that is close to the transition state for the water rocking motion relative to CN^-. The qualitative agreement between the calculated shift in the VDEs of 0.16 eV for the maximum of the probability for the $\upsilon = 2$ vibrational level relative to the C_s global minimum and the experimental observation (0.25 eV) further supports this conclusion. In a sense, the structure of $CN^-(H_2O)$ at RT is quite dynamic and the water molecule is likely roaming around the solute CN^-. The current study provides a vivid example, which demonstrates the interplay between temperature and the structures and dynamics of anionic aqueous clusters. It also shows the importance of the close coupling of state-of-the-art experiment and high level calculations in elucidating complex chemical phenomena.

Acknowledgment. We thank Prof. J. Laane and P. Jungwirth for useful discussions and suggestions. S.S.X. acknowledges financial support from the Alexander von Humboldt Foundation for a renewed stay at the Physics Department of the Technical University of Munich at Garching. This work was supported by the Division of Chemical Sciences, Geosciences and Biosciences, Office of Basic Energy Sciences, U.S. Department of Energy (DOE). Part of this work was performed at the Environmental Molecular Sciences Laboratory (EMSL), a national scientific user facility sponsored by DOE's Office of Biological and Environmental Research and located at Pacific Northwest National Laboratory, which is operated by Battelle for the DOE.

References and Notes

(1) Niedner-Schatteburg, G.; Bondybey, V. E. *Chem. Rev.* **2000**, *100*, 4059–4086.
(2) Wang, X. B.; Yang, X.; Nicholas, J. B.; Wang, L. S. *Science* **2001**, *294*, 1322–1325.
(3) Papanikolas, J. M.; Gord, J. R.; Levinger, N. E.; Rat, D.; Vorsa, V.; Lineberger, W. C. *J. Phys. Chem.* **1991**, *95*, 8028–8040.
(4) Steel, E. A.; Merz, K. M.; Selinger, A.; Castleman, A. W. *J. Phys. Chem.* **1995**, *99*, 7829–7836.

(5) Cabarcos, O. M.; Weinheimer, C. J.; Lisy, J. M. *J. Chem. Phys.* **1999**, *110*, 8429–8435.
(6) Blades, A. T.; Jayaweera, P.; Ikonomou, M. G.; Kebarle, P. *J. Chem. Phys.* **1990**, *92*, 5900–5906.
(7) Markovich, G.; Pollack, S.; Giniger, R.; Cheshnovsky, O. *J. Chem. Phys.* **1994**, *101*, 9344–9353.
(8) Lehr, L.; Zanni, M. T.; Frischkorn, C.; Weinkauf, R.; Neumark, D. M. *Science* **1999**, *284*, 635–638.
(9) Sanov, A.; Nandi, S.; Lineberger, W. C. *J. Chem. Phys.* **1998**, *108*, 5155–5158.
(10) Choi, J. H.; Kuwata, K. T.; Cao, Y. B.; Okumura, M. *J. Phys. Chem. A* **1998**, *102*, 503–507.
(11) Ayotte, P.; Weddle, G. H.; Kim, J.; Johnson, M. A. *J. Am. Chem. Soc.* **1998**, *120*, 12361–12362.
(12) Weber, J. M.; Kelley, J. A.; Nielsen, S. B.; Ayotte, P.; Johnson, M. A. *Science* **2000**, *287*, 2461–2463.
(13) Balbuena, P. B.; Johnston, K. P.; Rossky, P. J. *J. Phys. Chem.* **1996**, *100*, 2706–2715.
(14) Cabarcos, O. M.; Weinheimer, C. J.; Lisy, J. M.; Xantheas, S. S. *J. Chem. Phys.* **1999**, *110*, 5–8.
(15) Xantheas, S. S. *J. Phys. Chem.* **1996**, *100*, 9703–9713.
(16) Tobias, D. J.; Jungwirth, P.; Parrinello, M. *J. Chem. Phys.* **2001**, *114*, 7036–7044.
(17) Yarne, D. A.; Tuckerman, M. E.; Klein, M. L. *Chem. Phys.* **2000**, *258*, 163–169.
(18) Dorsett, H. E.; Watts, R. O.; Xantheas, S. S. *J. Phys. Chem. A* **1999**, *103*, 3351–3355. Ayotte, P.; Nielsen, S. B.; Weddle, G. H.; Johnson, M. A.; Xantheas, S. S. *J. Phys. Chem. A* **1999**, *103*, 10665–10669.
(19) Goyal, S.; Schutt, D. L.; Scoles, G. *Phys. Rev. Lett.* **1992**, *69*, 933–936.
(20) Nauta, K.; Miller, R. E. *Science* **1999**, *283*, 1895–1897.
(21) Gerlich, D. *Adv. Chem. Phys.* **1992**, *82*, 1–176.
(22) Boyarkin, O. V.; Mercier, S. R.; Kamariotis, A.; Rizzo, T. R. *J. Am. Chem. Soc.* **2006**, *128*, 2816–2817.
(23) Zhou, J.; Santambrogio, G.; Brümmer, M.; Moore, D. T.; Woste, L.; Meijer, G.; Neumark, D. M.; Asmis, K. R. *J. Chem. Phys.* **2006**, *125*, 111102−1-4.
(24) Wang, X. B.; Yang, J.; Wang, L. S. *J. Phys. Chem. A* **2008**, *112*, 172–175.
(25) Diken, E. G.; Headrick, J. M.; Roscioli, J. R.; Bopp, J. C.; Johnson, M. A.; McCoy, A. B.; Huang, X.; Carter, S.; Bowman, J. M. *J. Phys. Chem. A* **2005**, *109*, 571–575.
(26) Roscioli, J. R.; Diken, E. G.; Johnson, M. A.; Horvath, S.; McCoy, A. B. *J. Phys. Chem. A* **2006**, *110*, 4943–4952.
(27) Ikeda, T.; Nishimoto, K.; Asada, T. *Chem. Phys. Lett.* **1996**, *248*, 329–335.
(28) Wang, L. S.; Ding, C. F.; Wang, X. B.; Barlow, S. E. *Rev. Sci. Instrum.* **1999**, *70:*, 1957–1966.
(29) Wang, X. B.; Wang, L. S. *Rev. Sci. Instrum.* **2008**, *79*, 073108−1-8.
(30) Dunning, T. H., Jr. *J. Chem. Phys.* **1992**, *90*, 1007–1023. Kendall, R. A.; Dunning, T. H., Jr.; Harrison, R. J. *J. Chem. Phys.* **1992**, *96*, 6796–6806.
(31) Frisch M. J.; et al. *Gaussian 98*, revision A.9; Gaussian Inc.: Pittsburgh, PA, 1998.
(32) Kendall, R. A.; Aprà, E.; Bernholdt, D. E.; Bylaska, E. J.; Dupuis, M.; Fann, G. I.; Harrison, R. J.; Ju, J.; Nichols, J. A.; Nieplocha, J.; Straatsma, T. P.; Windus, T. L.; Wong, A. T. *Comput. Phys. Commun.* **2000**, *128*, 260–283. High Performance Computational Chemistry Group. *NWChem, A Computational Chemistry Package for Parallel Computers*, version 4.6; Pacific Northwest National Laboratory: Richland, WA, 2003.
(33) Hirata, S. *J. Phys. Chem. A* **2003**, *107*, 9887–9897.
(34) Purvis, G. D., III; Bartlett, R. J. *J. Chem. Phys.* **1982**, *76*, 1910–1918.
(35) Raghavachari, K.; Trucks, G. W.; Pople, J. A.; Head-Gordon, M. *Chem. Phys. Lett.* **1989**, *157*, 479–483.
(36) Fan, P. D.; Valiev, M.; Kowalski, K. *Chem. Phys. Lett.* **2008**, *458*, 205–209.
(37) Werner H. J.; Knowles P. J. MOLPRO, a package of ab initio programs; Amos, R. D., Bernhardsson, A., Berning, A., Celani, P., Cooper, D. L., Deegan, M. J. O., Dobbyn, A. J., Eckert, F., Hampel, C., Hetzer, G., Korona, T., Lindh, R., Lloyd, A. W., McNicholas, S. J., Manby, F. R., Meyer, W., Mura, M. E., Nicklass, Palmieri, A. P., Pitzer, R., Rauhut, G., Schütz, M., Stoll, H., Stone, A. J., Tarroni, R., Thorsteinsson, T., contributors.
(38) At intermediate temperatures, the $CN^-(H_2O)$ signals were unstable due to difficulties of operating the ion trap, preventing us from obtaining more detailed temperature-dependent data.
(39) Bradforth, S. E.; Kim, E. H.; Arnold, D. W.; Neumark, D. M. *J. Chem. Phys.* **1993**, *98*, 800–810.
(40) Huber, K. P.; Herzberg, G. *Spectra of Diatomic Molecules*; Van Nostrand Rheinhold: New York, 1979; Vol. IV.
(41) Barone, V. *J. Chem. Phys.* **1994**, *101*, 10666. Barone, V.; Adamo, C.; Minichino, C. *Theochem. J. Mol. Struct.* **1995**, *330*, 325. Minichino, C.; Barone, V. *J. Chem. Phys.* **1994**, *100*, 3717.
(42) Frisch, M. J.; et al. *Gaussian 03*, revision E.01; Gaussian, Inc.: Wallingford, CT, 2004.
(43) Laane, J. *Appl. Spectrosc.* **1970**, *24*, 73–80.
(44) Laane, J. *J. Phys. Chem. A* **2000**, *104*, 7715–7733.

JP9034002